IFSCC 2025 full paper (IFSCC2025-1082)

"Purification and Functional Evaluation of Exosome-like Nanoparticles Derived from Pavlova"

Shun Kimura [1], Nozomi Hirose [1], Xiang Long [1], Kaoru Mizutani[1], Yuya Hayashi[1], and Noriko Suenobu[1,*]

[1] Rohto Pharmaceutical Co., Ltd. Osaka, 544-8666

1. Introduction

Following minimally invasive aesthetic medical interventions, it is imperative to facilitate the prompt alleviation of adverse effects such as wounds, pain, and erythema, while concurrently promoting and regulating the reconstruction of skin tissue in a morphologically and functionally optimal manner. Exosomes derived from human cells, encapsulating growth factors and RNA, have been recognized for their pivotal role in sustaining human homeostasis through the mediation of intercellular communication. Notably, mesenchymal stem cell-derived exosomes exhibit well-established wound-healing properties, with their potential applications extending beyond medical therapies into the realm of skincare[1, 2]. Nevertheless, the utilization of human cell-derived substances demands stringent oversight concerning safety and quality assurance.

Plant-derived exosome-like nanoparticles (PELNs) possess the unique capability to mediate inter-kingdom communication and have been documented to exhibit a broad spectrum of bioactivities, including anti-inflammatory, antioxidant, antitumor effects, as well as the modulation of gut microbiota and immune homeostasis[3]. Within dermatological research, various PELNs have demonstrated functional properties: grapefruit-derived ELNs and wheat-derived ELNs have been shown to accelerate wound healing[4, 5]; cucumber-derived ELNs promote skin permeability of lipophilic actives [6]; ginseng-derived ELNs ameliorate dermal fibroblast senescence[7]; and *Dendropanax morifera*-derived ELNs exhibit melanogenesis-inhibitory effects[8].

Pavlova, a marine microalga that thrives under harsh ultraviolet radiation and osmotic stress conditions, is known to possess elevated concentrations of bioactive compounds, such as fucoxanthin, omega-3 fatty acids, and betaine lipids relative to other microalgal species, and has been harnessed as a functional food resource[9]. Utilizing cultivation systems incorporating deep-sea water and photobioreactors enables the sustainable production of *Pavlova*, effectively curbing CO_2 emissions and mitigating environmental impact.

In the present study, we focus on *Pavlova*, a sustainable and highly functional bioresource endemic to the main island of Okinawa, and report the isolation, purification, and functional characterization of *Pavlova*-derived ELNs (*Pav*-ELNs) in human skin cells.

2. Materials and Methods

2.1. Isolation and purification of Pav-ELNs

Cultivation residues of Pavlova sp., sourced from the main island of Okinawa, were subjected to thermal treatment at 105°C for 4 minutes, followed by centrifugation. The recovered supernatant was sequentially filtered through a 0.2 μm membrane and further concentrated using tangential flow filtration equipped with a 300 kDa hollow fiber membrane. Following concentration and purification with phosphate-buffered saline (PBS), the resultant sample underwent sterilization via filtration through a 0.22 μm membrane, thereby yielding the *Pav*-ELNs preparation.

2.2. Particle Size Measurement

The particle size distribution and concentration of nanoparticles within Pav-*ELNs were determined using the NanoSight NS300 (Malvern, UK).* Pav-*ELNs samples were diluted with PBS, introduced into the sample chamber, and irradiated with a 405 nm laser, with the resulting scattered light monitored for analysis.*

2.3. Lipidome analysis

Untargeted lipid profiling was performed by the Kazusa DNA Research Institute as reported previously[10].

2.4. Cell culture

Normal human epidermal keratinocytes (NHEKs) were purchased from KURABO Industries LTD (Osaka, Japan). The NHEKs were maintained in HuMedia-KG2 (KURABO). NHEKs were seeded into T-225 flasks and grown in a humidified atmosphere of 5% CO2 at 37 °C. Normal human dermal fibroblasts (NHDFs) were purchased from KURABO and were maintained in Dulbecco's modified Eagle's medium (FUJIFILM Wako Chemical Corporation, Kanagawa, Japan) that was supplemented with 10% foetal bovine serum (Biowest, Rue du Vieux Bour, Nuaillé, France), and 100 units mL−1 penicillin, 100 μg mL−1 streptomycin (Thermo Fisher Scientific, MA, USA). NHDFs were seeded in T-225 flasks and grown in a humidified atmosphere of 5% CO2 at 37 °C. Replicative senescence induced NHDFs were established by serially passaging NHDFs at passage 4 for an additional 21 passages in culture medium supplemented with or without 0.01% *Pav*-ELN.

2.5. Fluorescent immunohistochemistry

All samples were fixed with 4% paraformaldehyde phosphate-buffered solution (FUJIFILM Wako Chemical). After washing and blocking with 0.2% Triton X-100 / PBS containing 1% BSA, fluorescent immunostaining was conducted using anti-claudin-1 antibody (abcam, ab211737), Goat anti-Rabbit IgG (H+L) Cross-Adsorbed Secondary Antibody conjugated with Alexa Fluor™ 488, and Hoechst 33342 (Thermo Fisher Scientific). The stained samples were visualized using an LSM 900 confocal laser scanning microscope (Carl Zeiss).

2.6. RT-PCR

RNA from Pav-ELNs-treated cells was purified using the RNeasy mini kit (QIAGEN, Venlo, Netherlands). cDNA libraries were synthesized using ReverTra Ace qPCR RT Kit (TOYOBO, Osaka, Japan). Real-time PCR was performed on an Applied Biosystems QuantStudio 12K Flex (Thermo Fisher Scientific) using a SYBR Premix Ex Taq II (TaKaRa Bio, Shiga, Japan) or a TaqMan Gene Expression Assay system (Thermo Fisher Scientific). The expression level

of each target gene was normalized to GAPDH expression. The primer pairs used for real-time PCR are listed in Table 1 and 2.

Table 1. Primers for RT-PCR (Taqman probes)

Gene	Source	Cat#
GAPDH	Thermo Fisher Scientific	Hs02786624_g1
p16	Thermo Fisher Scientific	Hs00923894_m1
p21	Thermo Fisher Scientific	Hs00355782_m1

Table 2. Primers for RT-PCR (SYBR)

Gene	Forward	Reverse
Claudin-1	GCTTCTCTCTGCCTTCTGGG	TCACACGTAGTCTTTCCCGC
Claudin-4	TGGGGCTACAGGTAATGGG	GGTCTGCGAGGTGACAATGTT
Occludin	ACTTCAGGCAGCCTCGTTAC	GCCAGTTGTGTAGTCTGTCTCA
Filaggrin	TGAAGCCTATGACACCACTGA	TCCCCTACGCTTTCTTGTCCT

2.7. Senescence associated beta gal (SA β-gal) staining

Replicative senescence induced NHDFs were stained by Senescence detection kit (abcam, ab65351). Captured images were processed using ImageJ Fiji by first converting them to gray-scale, followed by binarization, to quantitatively assess the area stained by β-galactosidase.

3. Results

3.1. Characteristics of Pav-ELNs

To confirm the presence of exosome-like nanoparticles in our *Pav*-ELNs samples, particle size distribution and concentration were assessed.

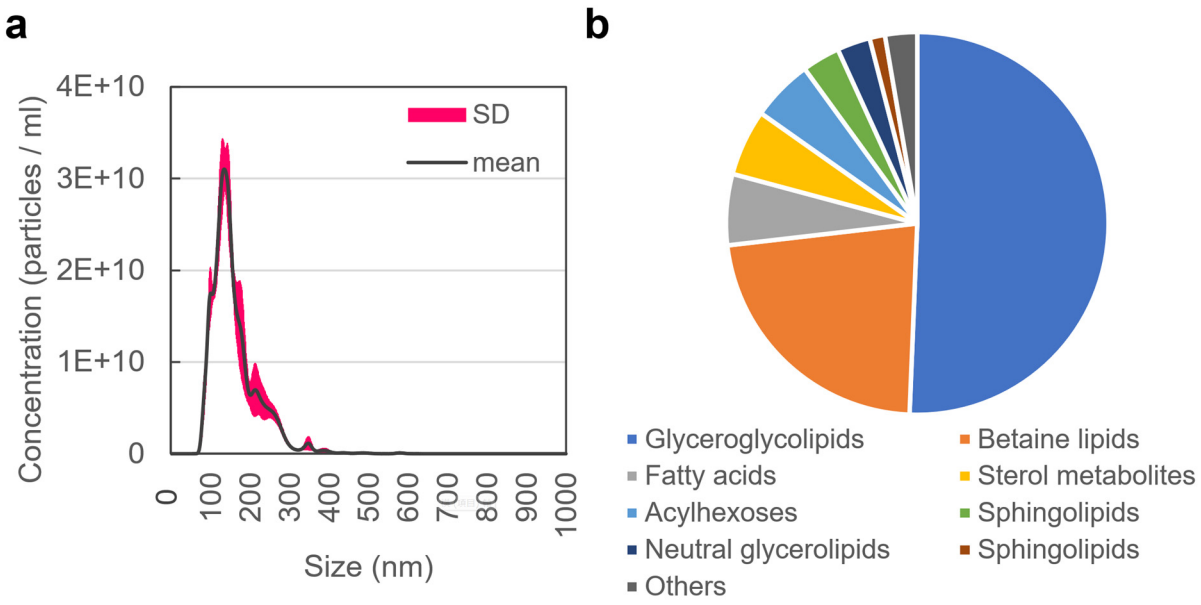

Figure 1. Characteristics of *Pav*-ELNs: (a) Analysis of particle size distribution and particle concentration of ELN particles contained in *Pav*-ELNs. (b) Unbiased lipidomic profiling of lipids contained in *Pav*-ELNs.

Analysis conducted with the NanoSight NS300 demonstrated that *Pav*-ELNs comprised a nanoparticle suspension with a concentration of 2.7×10^{12} particles/mL and an average particle diameter of 158.8 nm (Fig. 1a). Lipidomic analysis further revealed that *Pav*-ELN predominantly comprises lipids, including glyceroglycolipids, betaine lipids, fatty acids, sterol metabolites, and acylhexoses. Additionally, the presence of fucoxanthin and omega-3 fatty acids, characteristic components of *Pavlova*, was also indicated.

3.2. Pav-ELNs enhance Epidermal Keratinocyte Differentiation

To assess the epidermal efficacy of *Pav*-ELNs, NHEKs were treated with *Pav*-ELNs, and subsequent cellular morphological alterations were visualized through phase-contrast microscopy. Twenty-four hours post-treatment, the cells exhibited a relatively compact cobblestone-like morphology accompanied by the formation of dense intercellular junctions (Fig. 2a). This morphological adaptation mirrors the typical changes observed during NHEK differentiation under elevated calcium ion conditions, as previously documented[11]. Importantly, elemental analysis verified the absence of calcium ions within the *Pav*-ELNs preparations (Data not shown). RT-PCR-based gene expression profiling demonstrated that *Pav*-ELNs upregulated the expression of *Claudin-1*, *Claudin-4*, *Occludin*, and *Filaggrin* in NHEKs (Fig. 2b). Immunohistochemical analysis demonstrated that treatment of monolayer NHEK sheets with 1.5 mM calcium ions or 0.01% *Pav*-ELNs for 24 hours promoted the enhanced localization of Claudin-1 at intercellular junctions. Notably, combined treatment with both calcium and *Pav*-ELNs exhibited a synergistic effect, further intensifying the Claudin-1 signal (Fig. 2c).

3.3. Pav-ELNs ameliorate the progression of replicative senescence in NHDF

Given that *Pavlova* contains bioactive constituents such as phycocyanin and omega-3 fatty acids, recognized for their antioxidant and anti-inflammatory activities, we investigated the effects of *Pav*-ELNs on the progression of replicative senescence in NHDFs. NHDFs at passage 4 exhibited a spindle-shaped, relatively small morphology (Fig. 3a, upper left panel), whereas cells subjected to over 20 serial passages developed an enlarged, flattened morphology typical of senescent cells (Fig. 3a, upper center panel). In contrast, NHDFs continuously treated with 0.1% Pav-ELNs throughout the subculturing period retained well-defined cellular contours and exhibited a moderate suppression of cell enlargement (Fig. 3a, upper right panel). SA β-gal staining demonstrated that the increased SA β-gal positivity accompanying serial passaging was attenuated by 0.01% *Pav*-ELN treatment. Quantitative image analysis of SA β-gal-positive areas further substantiated the statistically significant suppression of SA β-gal activity by 0.01% *Pav*-ELNs (Fig. 3b). Furthermore, RT-PCR analysis revealed that 0.01% Pav-ELNs suppressed the passaging-induced upregulation of *p16* and *p21* gene expression (Fig. 3c). Collectively, these findings indicate that *Pav*-ELNs possess potential efficacy in mitigating cellular senescence in dermal fibroblasts.

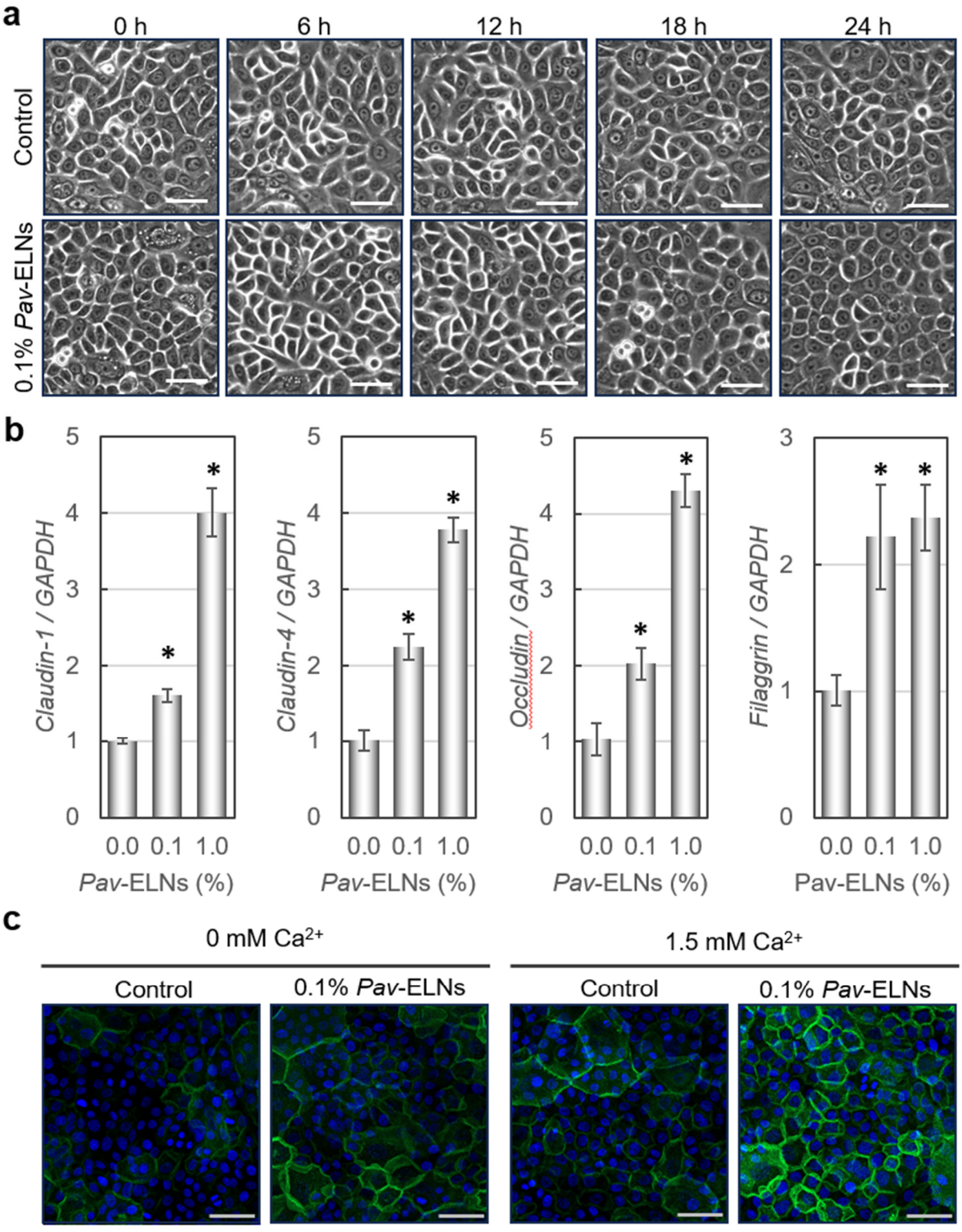

Figure 2. Pav-ELNs induce epidermal keratinocyte differentiation: (a) Time-dependent morphological changes of Pav-ELN-treated NHEK over a 24 h period. scale bar, 50 μm. (b) Real-time PCR analysis of keratinocyte differentiation and epidermal barrier-related genes of Pav-ELNs treated NHEK. *$P < 0.01$, as assessed by Dunnett's test following two-way analysis of variance (ANOVA; $P < 0.001$); error bars represent the standard deviation. (c) Immunohistochemical analysis of Claudin-1 distribution (Green). Scale bar, 20 μm.

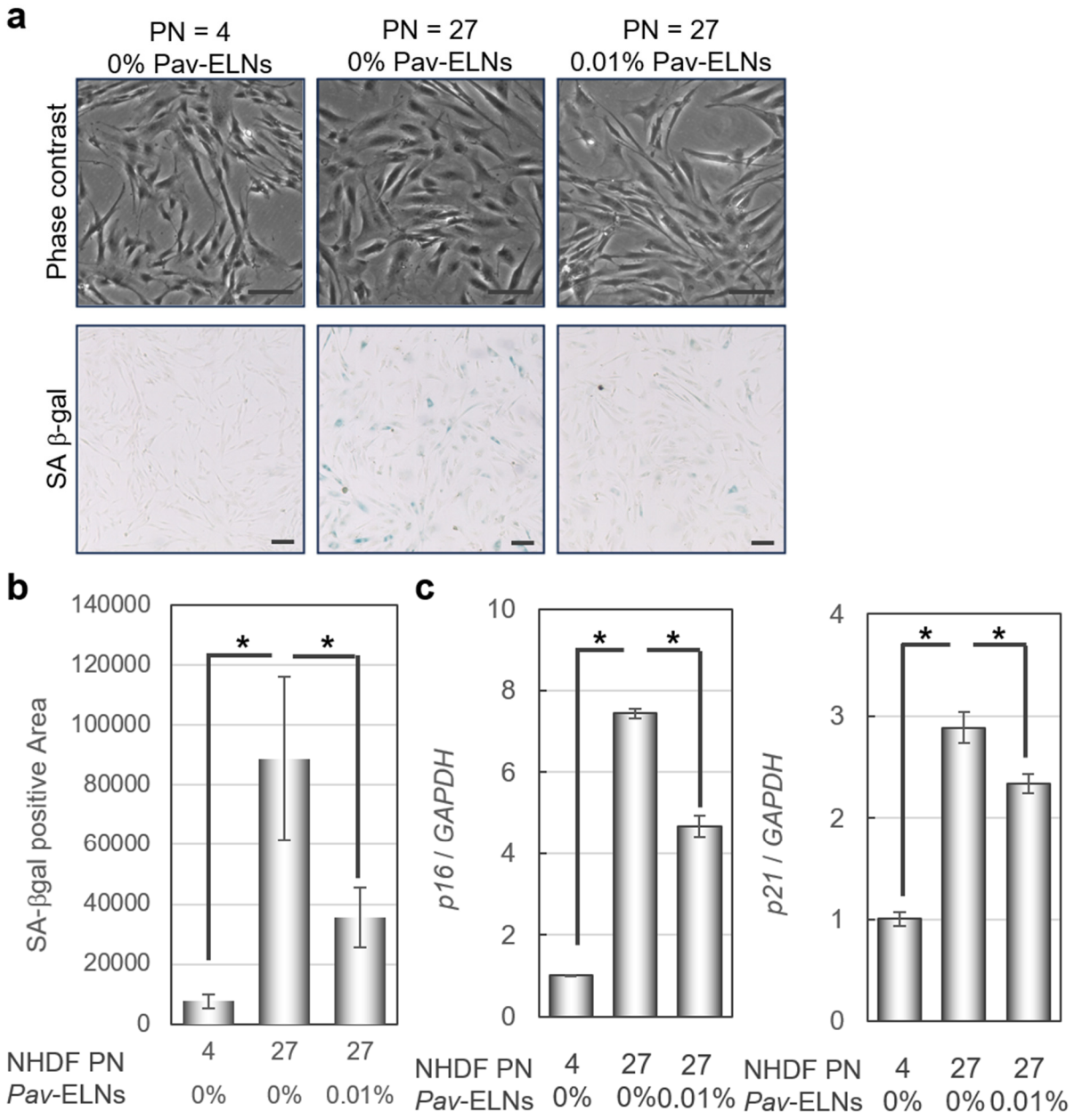

Figure 3. *Pav*-ELNs ameliorate the progression of replicative senescence in NHDF: (a) Morphological changes and SA β-gal activities of *Pav*-ELNs-treated NHDFs. scale bar, 100 μm. (b) Quantification of SA β-gal positive areas by image analysis. *P < 0.05, as assessed by two-tailed Student's t-tests; error bars represent the standard deviation. (c) Real-time PCR analysis of senescence associated genes of *Pav*-ELNs treated NHDFs. *P < 0.01, as assessed by two-tailed Student's t-tests; error bars represent the standard deviation.

3.4. Pav-ELNs promote type I collagen fiber formation in synergy with ascorbic acid derivative.

To investigate the potential efficacy of *Pav*-ELNs in dermis, we evaluated their influence on type 1 collagen fiber formation in NHDFs cultured with or without a vitamin C derivative. Under magnesium ascorbyl phosphate (MAP)-free conditions, *Pav*-ELNs demonstrated negligible effects on collagen fiber formation. In contrast, in the presence of MAP, *Pav*-ELNs markedly

promoted collagen fiber synthesis, with image analysis confirming that this enhancement was statistically significant.

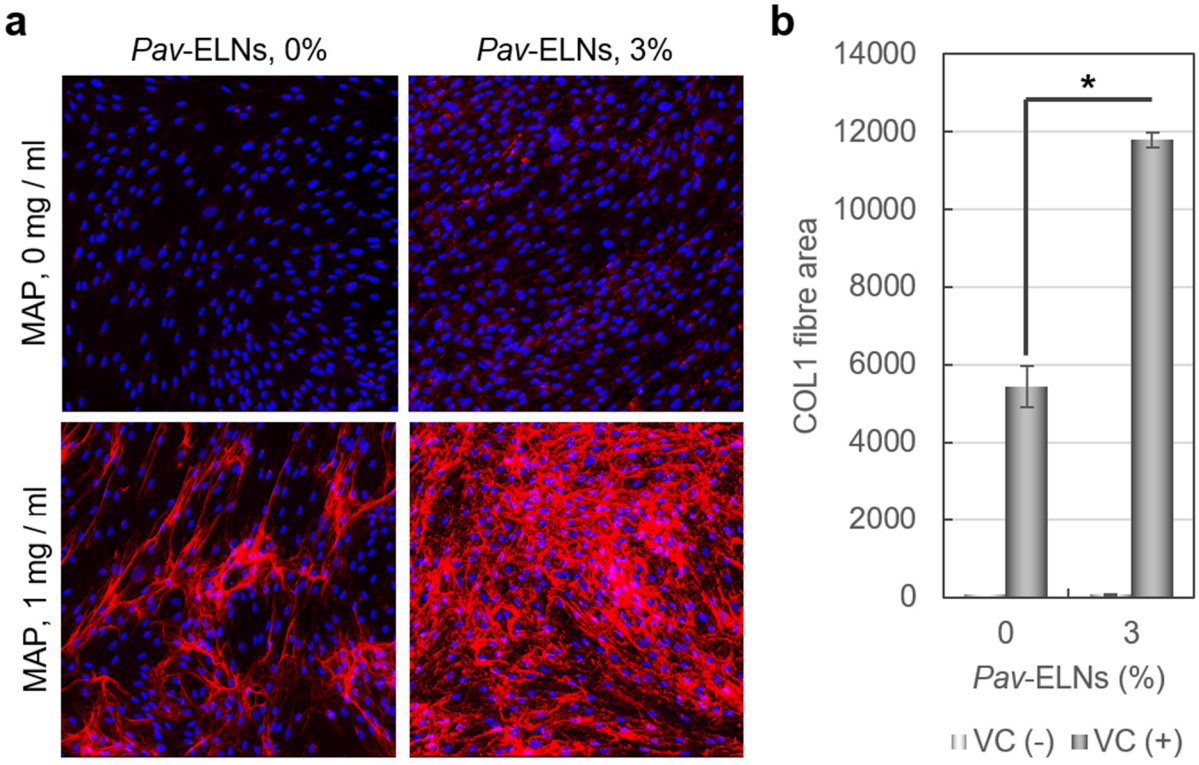

Figure 4. *Pav*-ELNs promote type 1 collagen fiber formation in synergy with ascorbic acid derivative: (a) Visualization of type 1 Collagen fiber formation (Red) by immunocytochemical analysis. (b) Quantification of type 1 collagen positive areas by image analysis. *$P < 0.01$, as assessed by Tukey–Kramer test following two-way analysis of variance (ANOVA; $P < 0.001$); error bars represent the standard deviation.

4. Discussion

In this study, we focused on *Pavlova*, a sustainable functional bioresource, and established methods for the extraction and purification of *Pav*-ELNs. Although the purification protocols and precise definition of PELNs remain under debate, our *Pav*-ELNs were identified as a concentrated nanoparticle solution, approximately 150 nm in diameter, enriched with lipids characteristic of *Pavlova*, such as betaine lipids and omega-3 fatty acids and phycocyanin. Given the inclusion of betaine lipids, which protect cells from osmotic stress, alongside the antioxidant and anti-inflammatory properties of omega-3 fatty acids and phycocyanin, we hypothesized that *Pav*-ELNs possess skin-beneficial properties, including moisturization and anti-senescence effects.

Functional evaluations in epidermal keratinocytes demonstrated that *Pav*-ELNs promote keratinocyte differentiation. These findings suggest that Pav-ELNs may contribute to the enhancement of epidermal barrier function. *Pav*-ELNs alone were sufficient to induce cellular morphological changes and upregulate differentiation-associated gene expression. However, co-treatment with calcium ions further augmented epidermal barrier function, as evidenced by increased Claudin-1 protein expression. As *Pav*-ELNs contain negligible calcium ions, these effects likely involve calcium-independent mechanisms, though the underlying pathways remain to be elucidated.

Functional assessments in dermal fibroblasts revealed that *Pav*-ELNs attenuate replicative senescence. Specifically, *Pav*-ELNs reduced SA β-gal staining and suppressed the expression of senescence-associated genes *p16* and *p21*. Nonetheless, comprehensive evaluation of additional senescence markers is warranted to substantiate these findings. Given the presumed anti-inflammatory properties of *Pav*-ELNs, further investigation into their mechanisms of action is necessary.

Furthermore, we found that *Pav*-ELNs alone exert minimal influence on collagen fiber formation but synergistically enhance collagen synthesis in combination with a vitamin C derivative. Since PELNs are anticipated to exhibit both intrinsic bioactivity and delivery capabilities, further studies focusing on collagen fiber maturation and intracellular vitamin C dynamics are essential to fully elucidate these mechanisms.

In conclusion, *Pav*-ELNs exhibit potential in improving epidermal barrier integrity and mitigating age-related changes in dermal cells and extracellular matrices by acting synergistically with endogenous factors such as calcium ions and vitamin C. The combination of *Pav*-ELNs with aesthetic procedures, including microinjection or laser treatment, may accelerate epidermal recovery and ameliorate aging phenotypes such as wrinkles and sagging. Additionally, advancing the mechanistic understanding of plant-derived ELNs could facilitate the enhancement of the biological efficacy of established functional ingredients, including vitamin C.

5. Conclusion

In this study, we established protocols for the extraction and purification of *Pav*-ELNs and elucidated their functional properties, including the enhancement of epidermal barrier formation, the mitigation of replicative senescence in dermal fibroblasts, and the synergistic promotion of collagen fiber formation in conjunction with vitamin C. *Pav*-ELNs are anticipated to augment the efficacy of anti-aging interventions when integrated with cosmetic procedures. Moreover, advancing the mechanistic understanding of PELNs and optimizing their development may facilitate the enhancement of existing skincare materials and theoretical paradigms.

6. References

[1] D. Bian, Y. Wu, G. Song, R. Azizi, and A. Zamani, “The application of mesenchymal stromal cells (MSCs) and their derivative exosome in skin wound healing: a comprehensive review,” Dec. 01, 2022, *BioMed Central Ltd*. doi: 10.1186/s13287-021-02697-9.

[2] A. Thakur *et al.*, “Therapeutic Values of Exosomes in Cosmetics, Skin Care, Tissue Regeneration, and Dermatological Diseases,” Apr. 01, 2023, *MDPI*. doi: 10.3390/cosmetics10020065.

[3] C. Bai *et al.*, “Research status and challenges of plant-derived exosome-like nanoparticles,” *Biomedicine & Pharmacotherapy*, vol. 174, p. 116543, May 2024, doi: 10.1016/j.biopha.2024.116543.

[4] Y. Savcı *et al.*, “Grapefruit-derived extracellular vesicles as a promising cell-free therapeutic tool for wound healing,” *Food Funct*, vol. 12, no. 11, pp. 5144–5156, 2021, doi: 10.1039/D0FO02953J.

[5] F. Şahin, P. Koçak, M. Y. Güneş, İ. Özkan, E. Yıldırım, and E. Y. Kala, “In Vitro Wound Healing Activity of Wheat-Derived Nanovesicles,” *Appl Biochem Biotechnol*, vol. 188, no. 2, pp. 381–394, Jun. 2019, doi: 10.1007/s12010-018-2913-1.

[6] A. M. Abraham *et al.*, “Cucumber-Derived Exosome-like Vesicles and PlantCrystals for Improved Dermal Drug Delivery,” *Pharmaceutics*, vol. 14, no. 3, Mar. 2022, doi: 10.3390/pharmaceutics14030476.

[7] E. G. Cho *et al.*, “Panax ginseng-derived extracellular vesicles facilitate anti-senescence effects in human skin cells: An eco-friendly and sustainable way to use ginseng substances,” *Cells*, vol. 10, no. 3, pp. 1–25, Mar. 2021, doi: 10.3390/cells10030486.

[8] R. Lee *et al.*, “Anti-melanogenic effects of extracellular vesicles derived from plant leaves and stems in mouse melanoma cells and human healthy skin,” *J Extracell Vesicles*, vol. 9, no. 1, Jan. 2020, doi: 10.1080/20013078.2019.1703480.

[9] J. K. Volkman, G. A. Dunstan, S. W. Jeffrey, and P. S. Kearney, “Fatty acids from microalgae of the genus Pavlova,” *Phytochemistry*, vol. 30, no. 6, pp. 1855–1859, 1991, doi: 10.1016/0031-9422(91)85028-X.

[10] Y. Endo *et al.*, “1-Oleoyl-lysophosphatidylethanolamine stimulates RORγt activity in T H 17 cells,” *Sci Immunol*, vol. 8, no. 86, Aug. 2023, doi: 10.1126/sciimmunol.add4346.

[11] L. Micallef *et al.*, “Effects of extracellular calcium on the growth-differentiation switch in immortalized keratinocyte HaCaT cells compared with normal human keratinocytes,” *Exp Dermatol*, vol. 18, no. 2, pp. 143–151, 2009, doi: 10.1111/j.1600-0625.2008.00775.x.